

A Tactile Recognition System Mimicking Human Mechanism for Recognizing Surface Roughness*

Masahiro OHKA**, Takuya KAWAMURA***, Tastyu ITAHASHI****, Jyun-ichi TAKAYANAGI†, Tetsu MIYAOKA†† and Yasunaga MITSUYA†††

A mathematical model was formulated on the basis of results from psychophysical experiments in which human subjects discriminated fine steps on aluminum plates. The mathematical model emulated the real neuron discharge caused when a membrane potential exceeds a threshold. This membrane potential was determined by spatial and temporal summations of postsynaptic potential. To evaluate the mathematical model for surface texture recognition by robots, we performed a series of surface-detection experiments using a robotic manipulator equipped with an optical three-axis tactile sensor. The single sensor cell of this sensor consisted of a columnar feeler and a 2-by-2 array of conical feelers. The three-axis force was calculated from the area-sum and area-difference of the conical feelers' contact areas. The robotic manipulator rubbed the tactile sensor on four brass plates with step heights of 0, 0.05, 0.1 and 0.2 mm. Results showed that the mathematical model could distinguish these step heights in real time.

Key Words: Robotics and Mechatronics, Measurement, Neural Network, Tactile Sensor, Psychophysics, Step-Height Recognition

1. Introduction

Human beings can recognize subtle roughness of surfaces by touching the surfaces with their fingers. Moreover, the surface sensing capability of human beings maintains a relatively high precision outside the laboratory. If we can implement the mechanisms of human tactile sensation to robots, it will be possible to enhance the robustness

of robotic recognition precision and also to apply the sensation to surface inspection outside the laboratory.

We have previously investigated the mechanism of roughness recognition in psychophysical experiments that used mechanical vibrations or abrasive papers as the stimuli⁽¹⁾⁻⁽⁴⁾. From these experiments, we determined that tactile receptors can perceive a mechanical vibration of 0.2 μm in amplitude and a 3 μm difference in particle diameter between aluminum oxide abrasive papers. In a subsequent paper, we determined the difference thresholds for a fine step height of 10 μm when the human subjects actively touched the fixed step heights and passively touched the moving step heights^{(2),(3)}. The difference thresholds for a 10 μm step height in the passive-touch experiment agreed approximately with those in the active-touch experiment. Therefore, it was found that the human ability to precisely discriminate step heights did not depend on their touching manner because the difference threshold meant detecting precision.

Next, we experimentally investigated the discrimination ability of human tactile sensation more precisely than in the previous papers by presenting human subjects with several fine step heights that were moved at different velocities⁽⁴⁾. In the experiments, step heights moved at cyclic

* Received 16th June, 2004 (No. 02-1127). Japanese Original: Trans. Jpn. Soc. Mech. Eng., Vol.69, No.682, C (2003), pp.1719-1725 (Received 6th September, 2002)

** Graduate School of Information Science, Nagoya University, Furo-cho, Chikusa-ku, Nagoya 464-8601, Japan.
E-mail: ohka@is.nagoya-u.ac.jp

*** Faculty of Engineering, Gifu University, 1-1 Yanagido, Gifu 501-1193, Japan

**** Nippon Sharyo, LTD., 1-1 Sanbonmatsu-cho, Atsuta-ku, Nagoya 456-8691 Japan

† Toyota Motor Co., 1 Toyota-cho, Toyota-city 471-8571, Japan

†† Faculty of Science and Technology, Shizuoka Institute of Science and Technology, 2200-2 Toyosawa, Fukuroi 473-8555, Japan

††† Graduate School of Engineering, Nagoya University, Furo-cho, Chikusa-ku, Nagoya 464-8603, Japan

rates of 20 and 40 mm/s by a computer-controlled step-height presentation device were presented as the stimuli, and six human subjects discriminated several pairs of the moving step heights. The pairs of stimuli were chosen from among step heights of 7.6 to 12.4 μm . The human subjects passively touched single pairs of moving step heights presented in random order in each trial and judged which step height was higher in the pair. From the human subject's responses, we obtained two important values. One is the *difference threshold*, which shows the distinctive sensitivity of human tactile receptors, while the other is *subjective equality*, which shows the strength of stimulus measured by human tactile receptors. We examined these values of step-height sensing under different scanning speeds for moving fine step heights. Consequently, it was found that human subjects feel the moving fine step height more strongly at high scanning speeds than at low scanning speeds.

In the present paper, we adopted the McCulloch-Pitts model⁽⁵⁾, which simulates characteristics of a real neuron, as a mathematical model incorporated in a robotic program to emulate mechanoreceptor on the basis of the authors' and the other researchers' experimental results. In this model, neurons are discharged when a membrane potential exceeds a threshold and the membrane potential is determined by spatial and temporal summation of the postsynaptic potential. To evaluate the mathematical model for surface texture recognition by robots, we performed a series of FEM analyses and substituted the calculated results into the mathematical model. Subsequently, we conducted a series of surface-detection experiments using a robotic manipulator equipped with an optical three-axis tactile sensor, in which the robotic manipulator rubs the tactile sensor on four brass plates with step heights of 0, 0.05, 0.1 and 0.2 mm. The vertical displacement rate obtained from the surface detection experiments was substituted into the mathematical model to calculate the neuron discharge. The results were used to determine whether or not variations in the calculated neuron discharge represented recognition of the fine step height.

2. Psychophysical Remarks for Formulation

Human tactile recognition ability has been examined using psychophysical experiments and microneurography. Consequently, mechanoreceptors of skin are classified into four types according to response speed and receptive field size⁽⁶⁾. In the present paper, we focus our discussion on FA I (First adapting type I unit) because FA I responds to surface roughness. In regard to remarks related to FA I obtained by the authors and other researchers, remarks used for the present formulation are summarized as follows:

- (1) FA I responds to the first-order differential coefficient of mechanical stimulus^{(7),(8)} varying with time.
- (2) Acquirable physical stimuli of FA I are surface

roughness of several tens of microns in amplitude, and mechanical vibration of several microns in amplitude and several tens of Hz in frequency⁽⁸⁾.

- (3) Human subjects feel moving fine step height more strongly at high scanning speeds than at low scanning speeds⁽⁴⁾.

- (4) The mechanoreceptors related to FA I are Meissner's corpuscles^{(7),(8)}.

3. Neuron Model

Neurophysiology studies have clarified that the mechanoreceptive units comprise a few mechanoreceptors accepting mechanical stimuli and a sensory nerve fiber transmitting sensory signals. In the present paper, a neuron processing the sensory signals is treated as an element of the unit in order to consider the unit as comprising mechanoreceptors, a sensory nerve fiber and a neuron in the brain. If we make a model of the tactile nerve system on the basis of neural network models, it is easy to incorporate the above-mentioned human tactile mechanism into robotics.

The McCulloch-Pitts model⁽⁵⁾ is adopted here as the mechanoreceptive unit, while the afore-mentioned remarks on human tactile sensations are formulated to obtain expressions of the fine surface roughness recognition mechanism.

Figure 1 shows a neural network related to the tactile sensory system. When mechanical stimuli are applied to the surface of the skin, the mechanoreceptors accept the stimuli and emit a voltage signal. The signal is transmitted to a dendrite extending from a neuron through a synaptic connection. The arrival of the output signal from the mechanoreceptor effects a change in the membrane potential inside neuron. If several signals from mechanoreceptors arrive almost simultaneously at the neuron, these signals are superimposed in the neuron and summation of

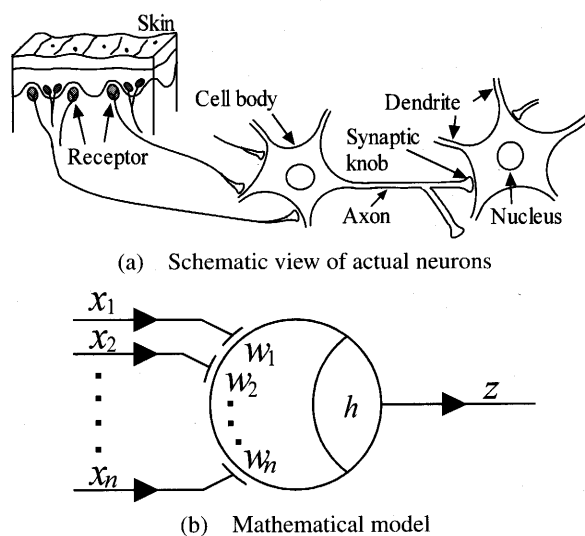


Fig. 1 Modeling of fast adaptive Type I mechanoreceptive unit

these signals change the membrane potential. This effect is called spatial summation and is modeled first.

The neuron accepts n -signals x_1, x_2, \dots, x_n emitted from n -mechanoreceptors distributed in the skin. The weight of the synaptic connection between i -th mechanoreceptor and the neuron is represented as w_i . Taking into account the spatial summation, the membrane potential, u is calculated as

$$u = \sum_{i=1}^n w_i x_i. \quad (1)$$

The mechanoreceptor seems to detect the time derivative of skin deformation according to Remark (1) in the previous section, where it is assumed that the mechanoreceptor detects the strain rate caused in the skin and that it emits signals proportional to the magnitude of the strain rate. Namely, the output of the i -th mechanoreceptor, x_i of Eq. (1) is calculated by the following expression,

$$x_i = a \left| \frac{d\varepsilon_i}{dt} \right|, \quad (2)$$

where ε_i is the compressive strain of the i -th mechanoreceptor and a is a coefficient.

When an output signal emitted from the mechanoreceptor arrives to the neuron, a change occurs in the membrane potential. If the next signal arrives at the neuron before the change attenuates and vanishes, the next signal is superimposed on the residual of the preceding signal. This effect is called *time summation*⁽⁹⁾ and is formulated as convolution integral of $w_i(t-t')x_i(t')$ with respect to t' from the past to the present t if the weight of synaptic connection between the i -th mechanoreceptor and the neuron is represented as $w_i(t')$ at time t' . Consequently, by incorporating the time summation into Eq. (1), the membrane potential u is calculated as

$$u = \sum_{i=1}^n \int_{-\infty}^t w_i(t-t')x_i(t')dt'. \quad (3)$$

Influence of signal arrival on the membrane potential decreases with late of the signal arrival. This effect is expressed as decreasing the synaptic potential, $w_i(t)$. However, there are no available data on variation in the synaptic potential. In the present paper, it is assumed that $w_i(t)$ varies as square wave; namely it takes a constant value during 0 to τ sec, after which it takes 0.

$$w_i(t) = \begin{cases} 1, & 0 \leq t < \tau \\ 0, & t < 0 \end{cases}. \quad (4)$$

It is known that neurons have the threshold effect where the neuron emits an output if the membrane potential, u expressed as Eq. (3), exceeds a threshold, h . The output is a pulse signal and the pulse density of the signal is proportional to the difference between membrane potential u and threshold h . The pulse density of the signal is expressed as z , while the threshold function, $\phi(q)$ is designated to formulate the threshold effect. The pulse density, z is,

$$z = \phi(u - h) \quad (5)$$

$$\phi(q) = \begin{cases} q, & q \geq 0 \\ 0, & q < 0 \end{cases}. \quad (6)$$

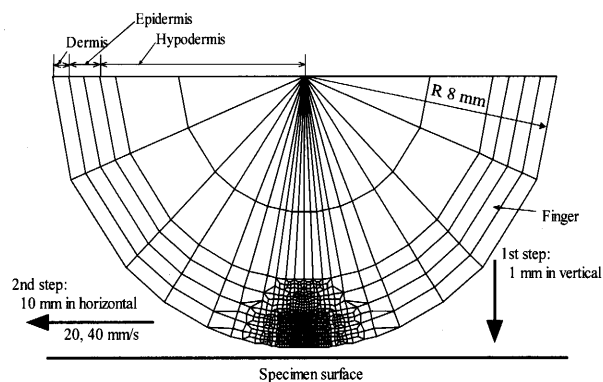
As mentioned above, data processing of the mechanoreceptive type FA I unit is formulated using a mathematical model for neuron-incorporated spatial and time summations. In the following sections, we confirm these expressions are by numerical simulation using FEM analysis of a human finger and experiments using an articulated robot installed in the present neural model.

4. Simulation

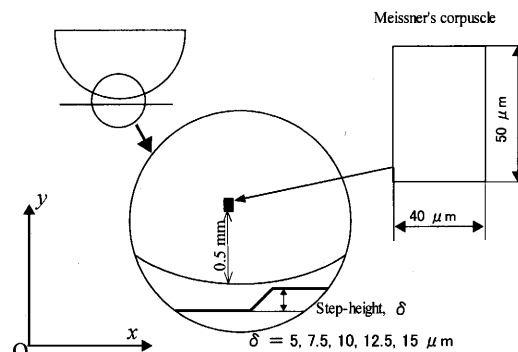
4.1 Calculated condition

As mentioned in Remark (4), the mechanoreceptor of FA I appears to be Meissner's corpuscle. In order to evaluate the present mathematical model derived in the preceding section, we performed a series of FEM analyses using a mesh model as shown in Fig. 2. In the present mesh model, a human finger is expressed as a half cylinder. Normal strain, ε_y arises at the existing portion of Meissner's corpuscle, calculated when the finger is slid along a flat surface having a fine step height. We selected $\delta = 5, 7.5, 10, 12.5$ and $15 \mu\text{m}$ as the step heights to compare experimental results obtained by psychophysical experiments.

It is possible that viscoelastic deformation of the skin causes the scanning speed effect described in Remark (3). In this paper, we adopt the first-order Prony series



(a) Mesh model



(b) Detail of the contact portion

Fig. 2 Mesh model for contact analysis

model⁽¹⁰⁾, which is equivalent to the three-element solid, as the viscoelastic model to approximate the skin's viscoelastic behavior.

Human skin is composed of three layers: the epidermis, the dermis, and the hypodermis. Young's moduli of these three layers are assumed to be 0.14, 0.034 and 0.080 MPa⁽¹¹⁾. On the other hand, the Poisson ratios of all layers are assumed to take same value of 0.45 because there are no reports concerned with it. Moreover, this value is reasonable if the skin has similar mechanical characteristics to rubber. Since there are no data on the ratio of the shearing modulus's initial value to its terminal value and the ratio between the bulk modulus' initial value and its terminal value for human skin, a common value of 0.5 for the three layers is assumed and a value of 12.9 msec⁽¹²⁾ is adopted as the time constant.

The present mesh model was compressed upon a flat rigid surface having a fine step height and slid over the surface. Then, we obtained the y -directional normal strain, ε_y in the Meissner's corpuscle, shown by a solid square in Fig. 2. The mesh element of Meissner's corpuscle is located 0.5 mm below the skin surface. The width and height of the element are 40 μm and 50 μm , respectively.

In the present loading history, the modeled finger was initially moved 1 mm in the negative perpendicular direction and compressed upon the flat surface. Subsequently, it was slid 10 mm in the horizontal direction. Any compressive deformation produced during the first step of the loading history should be diminished to allow evaluation of the stimulus of the fine step height caused by the scanning motion only. Therefore, after contact was established between the finger and the rigid flat surface, the finger was stabilized for 1 sec to diminish the effect of compressive deformation. Furthermore, we selected $v = 20$ mm/s and 40 mm/s for the finger sliding speed to simplify comparison between simulated and experimental results of psychophysical experiments conducted in our previous works. We selected 0 for the coefficient of friction between the finger and the rigid surface.

Next, we substituted the normal strain, ε_y obtained from the above-mentioned FEM analysis, into Eq. (2) by putting ε_y to ε_c . Subsequently, Eqs. (1)–(6) were calculated to obtain simulated signals emitted by FA I.

Although the constants included in Eqs. (1)–(4), a , n , τ and h should be determined by neurophysiological experiments, we could not obtain such data. We assumed the values of these constants as follows.

Here, a , the proportionality constant of relationship between output signal and stimulus magnitude, was presumed to be $a = 1$ Vsec. We were attempting to evaluate the simulation by normalizing outputs of the present model with the highest peak value among the outputs of different conditions. Since the plane strain condition was assumed in the present simulation, it was equivalent to a

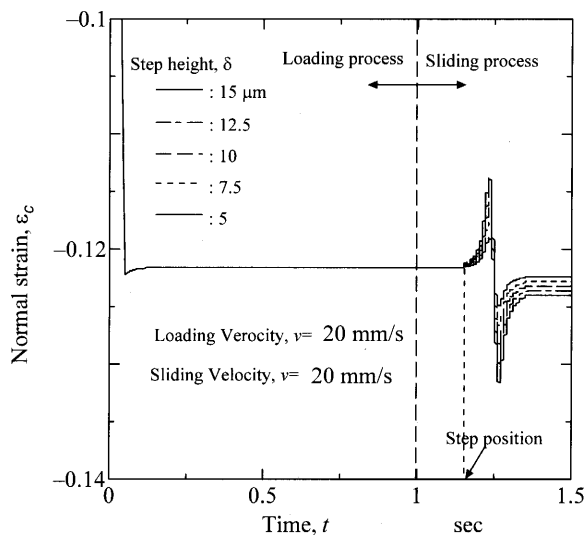


Fig. 3 Variation under compressive strain

simulation of Meissner's corpuscles aligned in the depth direction of this sheet and having the same characteristics. To abbreviate the present analysis, the variance among mechanoreceptive units was ignored and $n = 1$ was presumed. Since the afore-mentioned dependence of speed on step height recognition seems closely related to temporal summation, we calculated several time constants within a range of $\tau = 10 - 300$ msec. Following that, we selected the best τ that could best fit our experimental results. Since threshold h does not affect our simulated results, we summed $h = 0$ V.

4.2 Calculated result and discussion

Figure 3 shows the variation in normal strain of the position of Meissner's corpuscle as depicted in Fig. 2. Since the finger remains stationary for 1 sec to erase the history of the initial compressive strain, the variation remains at an almost constant value following the transient variation occurring at the initial stage. Then, when the fine step height comes near the position of Meissner's corpuscle, two prominent spikes arise. The figure also indicates that the magnitude of the spike increases with an increase in step height.

As mentioned in the previous section, we calculated several time constants within a range of $\tau = 10 - 300$ msec. First, we will examine variation in normalized pulse density at $\tau = 300$ msec. The strain rate calculated from the normal strain shown in Fig. 3 is substituted into the present mathematical model presented by Eqs. (1)–(6) to obtain the pulse density, z . Since we designated $a = 1$ as a value of the constant included in Eq. (2), the obtained pulse density z does not have any physical meaning. Hence, a comparison between calculated results under different conditions should be performed with a ratio. Here, the calculated pulse density is normalized as a peak of the calculated pulse density below $v = 40$ mm/s, and $\delta = 15$ μm is des-

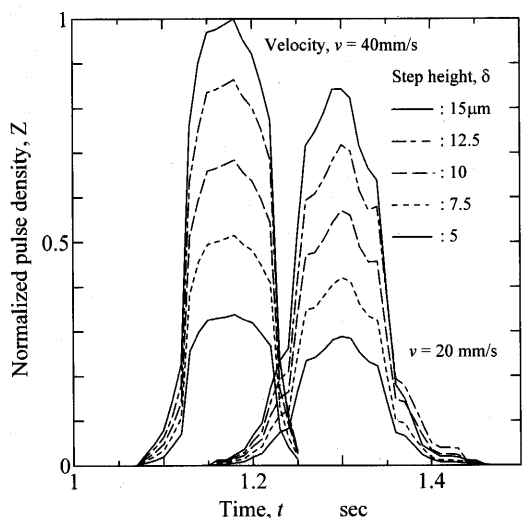


Fig. 4 Variation in normalized pulse density

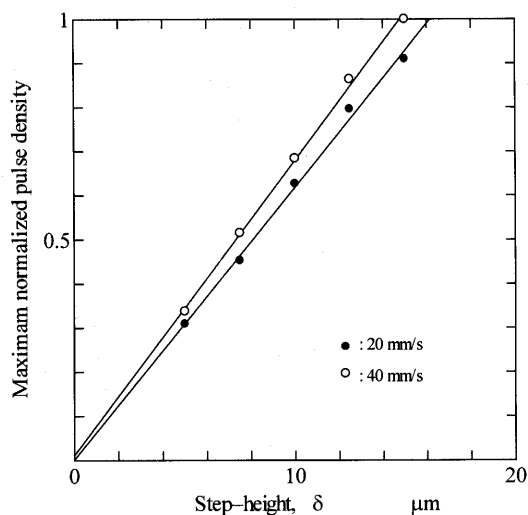


Fig. 5 Relationship between model output and step-height

ignated 1. In Fig. 4 the results are normalized according to the above-mentioned procedure.

For both $v = 20$ mm/s and 40 mm/s, results show that normalized pulse density increases with the reach of the mechanoreceptor to fine step heights, and that their maximum values increase with an increase in step height, δ . In order to examine the influence of a finger's sliding speed and step height on pulse density, we obtained the maximum value for each simulation condition. Figure 5 illustrates the relationship between maximum pulse density and step height for $v = 20$ mm/s and 40 mm/s.

The figure shows that the maximum pulse density is proportional to step height. If we compare pulse densities of different finger sliding speeds at the same step height to examine the influence of a finger's sliding speed on pulse density, we find the pulse density at a high finger speed is higher than at a low finger speed.

Next, to estimate a proper value of τ , we performed the same calculations (except for the value of τ) under the

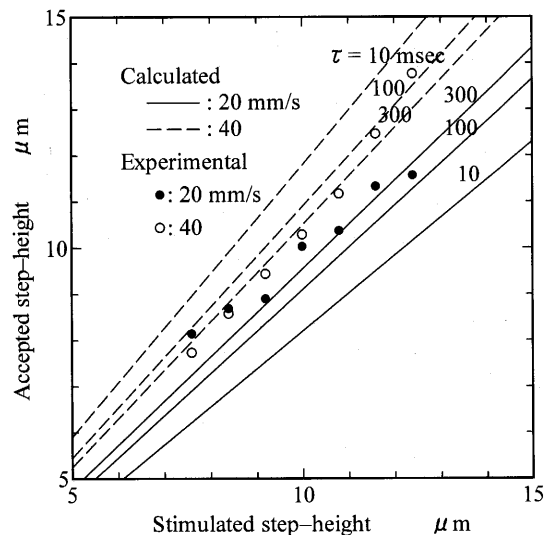


Fig. 6 Comparison of simulated results and experimental results

same calculation conditions as the calculation shown in Fig. 5. To obtain a conversion factor from the pulse density to the accepted step height, we obtained regression coefficients of calculated results for $v = 20$ and 40 mm/sec and adopted the mean value of the regression coefficient as the conversion factor. After employing this factor, the ordinate of Fig. 5 was transformed to an accepted step height, relationships between simulated step height and accepted step height were obtained, as shown in Fig. 6. The symbols in Fig. 6 show our experimental results⁽⁴⁾ obtained from a series of psychophysical experiments. This figure demonstrates that even if human subjects recognize the same step height, they feel that a given step height is higher at a high finger speed than at a low speed. Furthermore, on comparing calculated results with experimental results, we find that the calculated results coincide well with the experimental results below $\tau = 300$ msec.

5. Application to Robotics

5.1 Experimental apparatus and procedure

We used our three-axis tactile sensor^{(13),(14)} mounted on a robotic manipulator with five degrees of freedom. The robotic manipulator rubbed a brass plate with the tactile sensor's sensing surface. To enable the robotic manipulator to traverse the brass plate correctly, it is possible to adjust the horizontal datum of the brass plate with three screws attached to it at intervals of 120° . We prepared three brass plates having step heights of $\delta = 0.05$, 0.1 , 0.2 mm, and one brass plate having no step height ($\delta = 0$ mm).

The present tactile sensor features an array comprising tactile elements capable of sensing a three-axis force. The size and pitch between two adjacent tactile elements of the array are 10×13 and 3 mm, respectively. Since we obtained a transform matrix from the force vector to

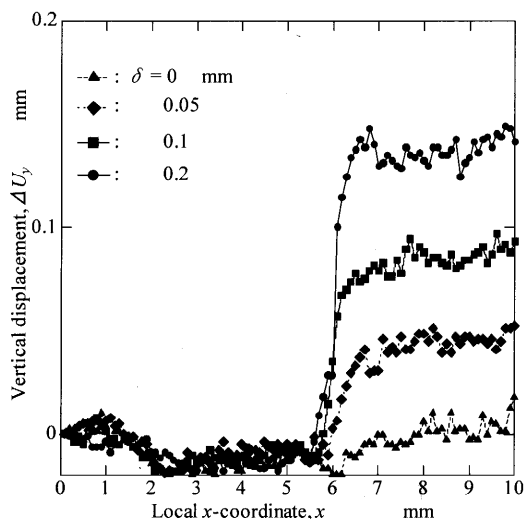


Fig. 7 Variation in vertical displacement

the displacement vector, the sensor could measure the displacement of the sensing element's tip. In the present experiment, we measured the vertical displacement of a sensing element located at the center of the array.

During the present experiment,

(1) we maintained contact between the tactile sensor's sensing surface and brass plate, and had the sensing surface press on the brass plate to apply an initial vertical force to the sensing element;

(2) the robotic manipulator traversed the brass plate in horizontal movement of 10 mm.

As a result, we obtained $\Delta U_y = U_y - U_{y0}$, which is the difference between the current vertical displacement and the initial vertical displacement, U_{y0} .

5.2 Experimental results and discussion

Figure 7 shows variation in the vertical displacement measured by the sensing element. The abscissa and ordinate of Fig. 7 are the local x -coordinates of the robotic manipulator's end-effector and the difference between the current vertical displacement and initial vertical displacement, ΔU_y , respectively. The origin of the abscissa corresponds to the position where the robotic manipulator applied the initial vertical force to the tactile sensor. Figure 7 shows that ΔU_y jumps at the step-height position, and that the jump heights increase with increasing step height. Furthermore, according to Fig. 7, the experimental results vary according to the step: if the step-height magnitudes of the experimental results are examined, it is found that the ratio is about 1:2:5, a ratio that approximates the ratio of the step heights formed on the brass plates (1:2:4). Therefore, the sensor can detect step heights formed on the surface of an object.

However, if we intend to measure the step height from variations in the vertical displacement U_y , then the initial displacement U_{y0} should be constant because it is used as a datum for step-height measurement. In the case of

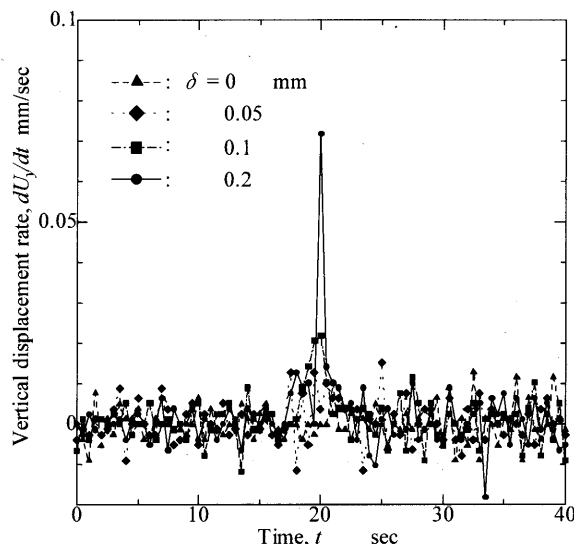


Fig. 8 Variation in rate of vertical displacement

robotics, the sensing surface of the tactile sensor often repeats touching and detaching from the object surface. Furthermore, there is no guarantee that the sensing surface faces parallel to the object surface; for step-height sensing, it is preferable that the step height is estimated from the current values.

As a candidate for the current physical quantity excluding the vertical displacement, U_y , we attempt to consider the time derivative of vertical displacement, \dot{U}_y . Figure 8 shows the variation in \dot{U}_y . The abscissa represents the time elapsed from begin of the scan just after initial load is applied. In Fig. 8, \dot{U}_y has a peak value corresponding to the position of step height. Since \dot{U}_y is determined from the current value obtained from the measurement, it appears more suitable than ΔU_y for robotic real-time step-height recognition, though it depends on the value of U_{y0} . However, since \dot{U}_y contains many noise components, it is difficult to discriminate step heights of $\delta = 0.05$ mm and 0.1 mm. Therefore, \dot{U}_y holds no advantage for fine discrimination of step height.

Next, the present model was incorporated into the robotic manipulator's surface-recognition system. The variation in the time derivative of vertical displacement of the present tactile sensor in Fig. 8, \dot{U}_y is divided by a representative length of the tactile sensor to obtain the strain rate substituted into Eq. (2). The strain rate becomes an input signal of the present model and is used to derive pulse density, z with Eq. (5). In this calculation, we employed the following constants included in the model: $a = 1$ Vsec, $n = 1$, $\tau = 3$ sec, $h = 0$ V.

In estimating the time constant, τ , we considered the difference of time consumption for data processing between human tactile sensation and robotic tactile recognition. Namely, since image-data processing is required to obtain tactile data in the present tactile sensor, sampling

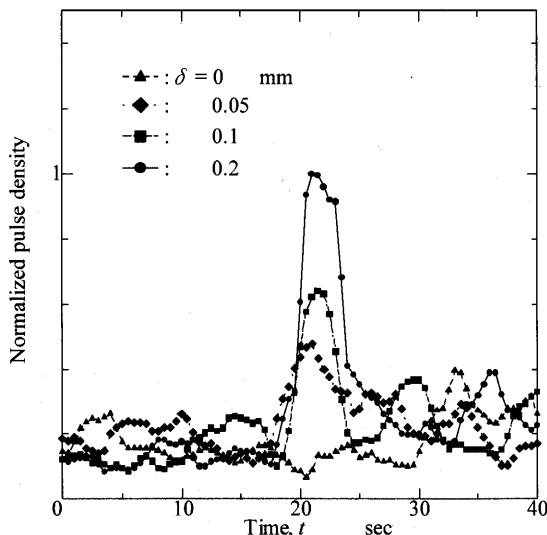


Fig. 9 Variation in pulse density

time is rather long at 0.5 sec. In contrast, FA I's band of tactile frequency is approximately several tens of Hz, and is one digit larger than the tactile sensor's band. Therefore, in calculating the present model, we used a value ten times larger than the $\tau = 300$ msec in Fig. 6.

Figure 9 illustrates the output of the present model. In this figure, the ordinate shows a normalized pulse density with its maximum value at a step height of 0.2 mm, while variation in the normalized pulse density, Z shows a single peak value. Furthermore, it is easy to distinguish the difference between the cases of $\delta = 0.05$ mm and 0.1 mm due to the noise-filtering effect of the present model. This discrimination was impossible in Fig. 8. As a result, we confirm that the present model is effective for robotic recognition of fine surface step heights in real time.

6. Conclusion

In the present study, a neuron model was presented for recognizing fine surface roughness on the basis of remarks in the fields of neurophysics and psychophysics in order to apply robust human recognition mechanism to robotics. In the present modeling, we modified the McCulloch-Pitts model with the incorporation of temporal summation to present dependence of scanning speed on step-height recognition. We assumed that the pulse density emitted from the mechanoreceptive unit is proportional to the magnitude of the strain rate occurring on human skin.

To evaluate the present model, we performed a series of simulations using mechanical contact analysis of finite elements (FEM). In the modeling, a mesh model was introduced to simulate a human finger. From the calculations, we obtained the skin's resulting strain rate and substituted it into the present model. Calculation results indicated that the pulse density calculated with the present model increases with an increase in the scanning speed of

the finger sliding along fine steps, regardless of steps being the same step height. This outcome agrees well with experimental results on human subjects.

Finally, we incorporated the present model into a robotic surface-recognition system. A robotic manipulator equipped with a tactile sensor scanned a flat plate with fine step height. The variation in pulse density showed a single peak value corresponding to step height. Furthermore, it was easy to distinguish the difference between the cases of $\delta = 0.05$ mm and 0.1 mm due to the noise-filtering effect of the present model. Therefore, it is confirmed that the present model is effective for robotic recognition of fine surface step heights in real time.

References

- (1) Miyaoka, T. and Ohka, M., Tactile Information Processing Mechanisms of Fine Surface Texture Discrimination in Humans: A Study with Ridge Height Discrimination Tasks, *Int. Ergonomics Association 13th Triennial Congress of the IEA, Vol.7 (1997)*, pp.264–266.
- (2) Kawamura, T., Ohka, M., Miyaoka, T. and Mitsuya, Y., Measurement of Human Tactile Sensation Capability to Discriminate Fine Surface Textures Using Variable Step-Height Presentation System, *Proc. of 5th IEEE Int. Workshop on Robot and Human Communication, (1996)*, pp.274–279.
- (3) Miyaoka, T., Mano, T. and Ohka, M., Mechanisms of Fine-Surface-Texture Discrimination in Human Tactile Sensation, *The Journal of the Acoustical Society of America, Vol.105, No.4 (1999)*, pp.2485–2492.
- (4) Kawamura, T., Ohka, M., Miyaoka, T. and Mitsuya, Y., Human Tactile Sensation Capability to Discriminate Moving Fine Texture, *Proceedings of IEEE RO-MAN'98 (IEEE International Workshop on Robot and Human Communication), (1998)*, pp.555–561.
- (5) McCulloch, W. and Pitts, W., A Logical Calculus of the Ideas Imminent in Nervous Activity, *Bulletin of Mathematical Biophysics, Vol.7 (1943)*, pp.115–133.
- (6) Vallbo, Å. B. and Johansson, R.S., Properties of Cutaneous Mechanoreceptors in the Human Hand Related to Touch Sensation, *Human Neurobiology, Vol.3 (1984)*, pp.3–14.
- (7) Moss-Salentijn, L., *The Human Tactile System, Advanced Tactile Sensing for Robotics*, Edited by Nicholls, H.R., (1992), pp.123–145, World Scientific Publishing.
- (8) Miyaoka, T., *Module Mechanisms in Tactile Sensation, Bulletin of Shizuoka Institute of Science and Technology, (in Japanese), Vol.3 (1994)*, pp.15–28.
- (9) Amari, T., *Mathematics of Neural Networks, (in Japanese), (1978)*, Sangyo-Tosho.
- (10) ABAQUS Theory Manual (Ver.5-7), (1998), pp.4.72.1–10.
- (11) Maeno, T., Kobayashi, K. and Yamazaki, N., Relationship between the Structure of Human Finger Tissue and the Location of Tactile Receptors, *Bulletin of JSME International Journal, Vol.41, No.1, C, (1998)*, pp.94–100.

- (12) Oka, H. and Irie, T., Bio-Mechanical Properties for Soft Tissue Modeling, Biomechanism, (in Japanese), Vol.17-4 (1993).
- (13) Ohka, M., Mitsuya, Y., Takeuchi, S. and Kamekawa, O., A Three-Axis Optical Tactile Sensor (FEM Contact Analyses and Sensing Experiments Using a Large-Sized Tactile Sensor), Proc. 1995 IEEE Int. Conf. on Robotics and Automation, (1995), pp.817-824.
- (14) Ohka, M., Mitsuya, Y., Matsunaga, Y. and Takeuchi, S., Sensing Characteristics of an Optical Three-Axis Tactile Sensor under Combined Loading, Robotica, Vol.22 (2004), pp.213-221.
-